Characterization of the continuous transition from atomic to molecular shape in the three-body Coulomb system

Laura D. Salas ⬤, Bárbara Zamora-Yusti ⬤,* and Julio C. Arce ⬤†

Departamento de Química, Universidad del Valle, A.A. 25360, Cali, Colombia

We present an alternative, univocal characterization of the continuous transition from atomic to molecular shape in the Coulomb system constituted by two identical particles and a third particle with the opposite charge as the mass ratio of the particles varies. Applying a marginal-conditional exact factorization to a variationally optimized wave function, we construct a nonadiabatic potential-energy surface for the relative motion between the single particle and each of the identical particles in the ground state. The transition is revealed through the evolution with the mass ratio of the topography of such a surface and of the shapes of the associated marginal and conditional distributions. Our approach unifies and extends to the nonadiabatic regime the Born-Oppenheimer and charge-distribution pictures of molecular shape.

I. INTRODUCTION

At present, thanks mainly to Woolley's early discussion, it is widely recognized that the justification of the so-called molecular structure hypothesis, i.e., the paradigm of modeling an isolated molecule as a semirigid three-dimensional array of atoms held together by chemical bonds, inherited from the classical structural theory of chemistry, is problematic for a fully *ab initio* quantum-mechanical theory of molecules [1–17]. This problem stems from the facts that the molecular Hamiltonian is entirely and uniquely specified just by the masses, charges, and spins of all the constituent nuclei and electrons, without any *a priori* reference to atoms, bonding, or geometry, and that the molecular wave function must exhibit the appropriate permutation symmetry for all subsets of indistinguishable particles [1,10,12–14,17,18]. Thus, *prima facie*, to recover such a classical-like description of molecular structure, auxiliary considerations must be added to the fully quantal treatment [1,2,4,9,10,13,14,17].

In quantum chemistry, the notion of a classical-like atomic arrangement, commonly called the molecular shape [2,11], is recovered from the topography of the Born-Oppenheimer (BO) potential-energy surface (PES) [13,14], whose isolated minima *define* the geometries of the nuclear frameworks of all the isomers allowed by the molecular formula. Clearly, this procedure does not *explain* the molecular shape since this property is not derived from first principles but is, instead, introduced in a semiempirical manner by presupposing that the nuclei are distinguishable and largely localized [1,10,13,14].

Taking for granted the BO approximation, an otherwise first-principles method for defining atoms and their bonding in molecules was presented by Langhoff and coworkers (see Ref. [15] and references therein). Hence, there remains the challenge of clarifying to what extent and under what conditions the molecular shape *emerges* [19] in the first place from a fully *ab initio* theory, which treats nuclei and electrons on equal footing [1,2,4,6,9,10,16].

Two main viewpoints about this "molecular-structure conundrum" [7,8] have been advanced. First, molecular shape is an intrinsic property (i.e., it can be attributed to the isolated system) that either arises only in nonstationary states, in compliance with position-energy complementarity [1,2], or emerges in a stationary state from the correlations between all the constituent particles [4,5,20,21] or originates from the decoherence induced on the nuclei by their interaction with the electrons [22,23]. Second, molecular shape is an extrinsic property; that is, it either is manifested only when the system is considered together with its environment, as a broken-symmetry phenomenon [1,2,10], or arises from the decoherence induced by the environment on the entire system [24] or is actualized by the act of measurement performed on the system by an observer [25]. Since this problem is intimately related to the classical limit of quantum mechanics, where the quantum peculiarities of particle delocalization, indistinguishability, and entanglement disappear, and even to the measurement process, both of which remain unclear [26,27], some authors are still pessimistic about the possibility of a complete bottom-up solution [16,17,28].

This work pursues a less ambitious goal, namely, a fully *ab initio* characterization of the transition from an atomlike to moleculelike shape in an isolated system in a stationary state without invoking any internal decoherence mechanism. We focus on the simplest system for which the property of molecular shape can be meaningfully ascribed, namely, three particles interacting through Coulomb forces, with two of

---

them being identical and the other one having the opposite charge, in the nonrelativistic ground state [20,21,29].

Since, strictly speaking, the ordinary notion of shape cannot be attributed to a quantal object [1,2,4,6–11,16,17], we had better begin by explaining what we mean by shape in this context. In Sec. II we make a critical assessment of a notion commonly adopted in the literature [5,20,21,29] and then expound, in qualitative terms, on a view that we believe to be more appropriate in general. Then, in Sec. III A we apply this view to the three-particle system, exploiting the marginal-conditional exact factorization (MCEF) of the eigenfunction introduced earlier [30].

It may be considered a disadvantage of such "pre-BO" [31] treatment that it has no place for a PES [13,14], such a construct being very useful as an interpretive tool. In fact, in Ref. [30] we showed that an exact nonadiabatic PES (NAPES) [3,32–35] can be rigorously constructed *for the electrons* in the He atom and that it has interpretive power, in particular for making connections with classical structure ideas. In Sec. III B we apply this development to the three-particle system, which allows us to treat atoms and molecules on the same basis, complementing and enriching the discussion on the emergence of molecular shape.

In Sec. IV we implement our formalism for sequences of realistic (from H^- to H_2^+) and model three-particle systems. As in Refs. [20,21,36,37], we examine the evolution of the system shape with the mass ratio of the single and double particles, which allows us to provide an alternative, univocal characterization of the transition from the atomlike to moleculelike shape.

We close with Sec. V, where we provide concluding remarks and perspectives for future developments in this line of work.

II. THE NOTION OF SHAPE FOR A QUANTAL SYSTEM

Since we can attribute the shape of a classical (macroscopic) object ultimately to the spatial distribution of its constituents in three-dimensional physical space, it may seem fitting to do the same for a quantal system [5,38]. Such a quantity is encoded in the spatial probability density, obtained by marginalizing, i.e., integrating over, the spin variables in the squared modulus of the eigenfunction in the position representation. However, if the system has N particles and their coordinates are defined with respect to a laboratory frame, the domain of this density will be a $3N$-dimensional configuration space. If the overall spatial translation is eliminated by a transformation to a space-fixed frame, as usual, the domain of this density will be a $(3N - 3)$-dimensional configuration space [18].

According to García-Sucre and Bunge [5], the particle distribution in physical space can be constructed from the one-particle marginal probability densities defined by marginalizing the spatial probability density over the coordinates of all the particles but one,

$$\rho_i(\vec{q}) = \int{}' d^{3N-6}q' |\Phi(\vec{Q})|^2, \qquad (1)$$

where $\vec{Q}$ is a $(3N - 3)$-vector containing all the coordinates, $\vec{q}$ is a three-vector, and the prime indicates that the integral

is to be performed over the configuration space that excludes the coordinates of the ith particle. Naturally, if the system contains a subset of indistinguishable particles, their one-particle marginal densities will be identical. The maxima of one such density will indicate the most probable positions of the particle in physical space. Alternatively, instead of the one-particle marginal densities the extracule densities, which have a similar interpretation but are defined in a different way employing a reference point, commonly the center of mass, can be utilized [20,21,29,39]. For a state with zero total angular momentum (S state) each maximum will actually constitute a two-dimensional spherical shell centered at the center of mass [20,29] due to the invariance of the Hamiltonian to overall spatial rotation [18]. These shells, considered independently, can provide partial information about the shape of the system. For example, for three-particle systems Mátyus and coworkers showed that a cut of the extracule density for the two identical particles is sufficient to characterize the transition from the atomic to molecular shape [20,21]. (Nevertheless, Ludeña and coworkers demonstrated that the shape of the extracule density depends on the reference point selected for its definition, leaving a degree of ambiguity [36,37].) The particle distribution is then obtained with [5]

$$\rho(\vec{q}) = \sum_{i=1}^{N} \rho_i(\vec{q}), \qquad (2)$$

which fulfills $\int d^3q \rho(\vec{q}) = N$ if Φ is normalized to 1. According to the analysis of García-Sucre and Bunge, the set of maxima of this density can be taken to define the shape of the system. In particular, for a semirigid molecule the set of regions of high nuclear density presumably correspond to the familiar ball-and-stick model. This view overlooks the rotational invariance of the Hamiltonian and, with that, the fact that the shells associated with the maxima in the one-particle densities of several particles can strongly overlap (for an example see Ref. [21]). This problem could be dealt with by a transformation to a molecule-fixed frame, albeit at the cost of considerable complication [12,18]. In any case, the one-particle densities can have several maxima, causing all the possible nuclear arrangements to be mixed up in the particle distribution, confounding the identification of the different structural isomers. Hence, such a prescription does not work in general.

A generally unambiguous concept of shape is straightforward if we return to the original spatial probability density in $(3N - 3)$-dimensional configuration space [4]. The maxima of this function will correspond to relatively likely configurations. We will refer to the arrangement of such maxima in the configuration space as the *quantal shape* of the system. For simplicity, let us now focus on S states. The nuisance of the overall rotation can be avoided by employing, from the start, the interparticle distances as a set of internal coordinates [40–43], which define a relative configuration space of dimension dim $= N(N - 1)/2$, in terms of which the Hamiltonian is cast automatically into a form manifestly invariant to overall translation, overall rotation, and coordinate inversion. (The remaining symmetries of the full symmetry group of the Hamiltonian are the permutations of the space and spin coordinates within all subsets of identical particles [18].) But still,

even for a three-particle system (dim $= 3$), the spatial probability density will be too complicated, making its analysis cumbersome. Therefore, it will be convenient to marginalize a chosen set of internal coordinates to obtain a reduced probability density in a relative configuration space of lower dimension, which is more amenable to visualization [4]. If this set is chosen judiciously, the shape of the system can still be characterized univocally.

For example, in the case of a molecule with N_n nuclei, marginalization of all the electron-electron and nucleus-electron distances from the full probability density will yield a purely nuclear probability density in a relative configuration subspace of dim $= N_n(N_n - 1)/2$. Now, the quantal *molecular* shape can be defined as the arrangement of the maxima of this function in the relative nuclear configuration subspace. Since each maximum defines a nuclear framework corresponding to the classical shape of a possible structural isomer, the quantal molecular shape comprises all the possible classical molecular shapes. (However, note that the correspondence is not necessarily one-to-one. For one thing, if enantiomers are possible, there will be one maximum associated with every *pair* of them. Due to the invariance of the internal Hamiltonian to coordinate inversion, the eigenfunction can be chosen to have definite positive or negative parity. In that case, such a maximum will correspond to the configuration of a superposition of both enantiomers with positive or negative parity. This issue is related to the so-called Hund's paradox [1,27]. Furthermore, if the molecule contains indistinguishable nuclei, several configurations arising from the permutations of such nuclei will correspond to one classical shape.) The form and breadth of a maximum will contain the information about the natures and amplitudes of the distortions ("vibrations") of the entire corresponding nuclear framework. This notion of quantal molecular shape in $N_n(N_n - 1)/2$ relative nuclear configuration subspace conforms with what Claverie and Diner call "quantum structure" [4] and should be contrasted with the classical structure usually depicted as a ball-and-stick cartoon, sometimes with the balls replaced by thermal ellipsoids to represent the anisotropic vibrations [38]. Nevertheless, the conundrum of why only one of the structural or optical isomers is observed in chemical experiments, which has elicited so much debate in the literature [1,2,4,6–11,16,17,19,25,27,28], still remains.

III. THE MARGINAL-CONDITIONAL EXACT FACTORIZATION FORMALISM

A. The quantal shape of the three-particle system

Let us now specialize these ideas to our three-particle system. We consider the charges $q_1 = q_2 = -q_3$ (according to charge conjugation invariance, it is immaterial whether q_3 is positive or negative). Thus, the masses $m_1 = m_2 < m_3$ model an atomlike system, with the identical particles playing the role of the electrons, whereas the masses $m_1 = m_2 > m_3$ model a moleculelike system, with the identical particles playing the role of the nuclei. The only symmetry of the Hamiltonian that needs explicit consideration is the permutation of the spatial and spin coordinates of particles 1 and

2. We assume that these particles are fermions, so that the eigenfunction must be antisymmetric under this operation.

For an S state the internal coordinates are r_{12}, r_{13}, r_{23}, where r_{ij} is the distance between particles i and j [40–43]. They determine the shape and size of the triangle defined by the positions of the three particles and are independent, except that they are constrained by the triangle condition $|r_{13} - r_{23}| \leqslant r_{12} \leqslant r_{13} + r_{23}$. The volume element of this configuration space is $dV = r_{12}r_{13}r_{23}dr_{12}dr_{13}dr_{23}$.

The eigenfunction can be written as the product of a spatial part, $\Phi(r_{12}, r_{13}, r_{23})$, and a spin eigenfunction which, in turn, is the product of a spin function for particles 1 and 2 and a spin function for particle 3 [44]. Evidently, in this case the marginalization of the spin variables in the probability density amounts to working only with the spatial eigenfunction since the spin eigenfunction is normalized. Hence, the quantal shape of this system is encoded in the joint distribution function

$$D(r_{12}, r_{13}, r_{23}) = r_{12}r_{13}r_{23}|\Phi(r_{12}, r_{13}, r_{23})|^2 \qquad (3)$$

(which includes the Jacobian because it is a radial probability density). We marginalize the distance between the identical particles r_{12} to obtain a two-dimensional marginal distribution (MD) for finding particles 1 and 2 at distances r_{13} and r_{23} from particle 3, respectively, *regardless* of r_{12} (here and henceforth, when we speak of the probability of finding two particles at a certain distance, we mean within an infinitesimal neighborhood around that distance),

$$D_m(r_{13}, r_{23}) := \int_{|r_{13}-r_{23}|}^{r_{13}+r_{23}} dr_{12}r_{12}D(r_{12}, r_{13}, r_{23}). \qquad (4)$$

Note that if we marginalized two of the distances, we would obtain a one-dimensional MD that obviously could not provide, by itself, information about the shape of the system. Now, according to Bayes's product rule, the joint distribution can be factorized exactly as

$$D(r_{12}, r_{13}, r_{23}) = D_m(r_{13}, r_{23})D_c(r_{12}|r_{13}, r_{23}), \qquad (5)$$

where D_c is the conditional distribution (CD) function for finding particles 1 and 2 at a distance r_{12}, *provided* they are found at distances r_{13} and r_{23} from particle 3, respectively. Taking into account the normalization of D,

$$\int_0^\infty dr_{13}r_{13} \int_0^\infty dr_{23}r_{23}$$
$$\times \int_{|r_{13}-r_{23}|}^{r_{13}+r_{23}} dr_{12}r_{12}D(r_{12}, r_{13}, r_{23})$$
$$= 1, \qquad (6)$$

and imposing that D_m be normalized in the $\{r_{13}, r_{23}\}$ configuration subspace,

$$\int_0^\infty dr_{13}r_{13} \int_0^\infty dr_{23}r_{23}D_m(r_{13}, r_{23}) = 1, \qquad (7)$$

imply that D_c is *locally* normalized at every point of this subspace,

$$\int_{|r_{13}-r_{23}|}^{r_{13}+r_{23}} dr_{12}r_{12}D_c(r_{12}|r_{13}, r_{23}) = 1. \qquad (8)$$

When evaluated at selected points (r_{13}, r_{23}), the CD becomes a one-dimensional function that can also aid in the analysis. (It is worth mentioning that Berry and coworkers have employed two-dimensional CDs defined in an *ad hoc* way by fixing the distance between one electron and the nucleus in the joint distribution to illustrate that two-valence-electron atoms acquire a moleculelike shape in some states [45].)

B. The nonadiabatic potential-energy surface

The structure of our nonrelativistic three-particle system in an S state is governed by the internal Schrödinger equation [40–43]

$$\hat{H}\Phi(r_{12}, r_{13}, r_{23}) = E\Phi(r_{12}, r_{13}, r_{23}). \tag{9}$$

In atomic units ($\hbar = m_e = e = 1$), the spin-free Hamiltonian reads [42,43]

$$\hat{H} = -\frac{1}{2\mu_{12}}\left(\frac{\partial^2}{\partial r_{12}^2} + \frac{2}{r_{12}}\frac{\partial}{\partial r_{12}}\right) - \frac{1}{2\mu_{13}}\left(\frac{\partial^2}{\partial r_{13}^2} + \frac{2}{r_{13}}\frac{\partial}{\partial r_{13}}\right) - \frac{1}{2\mu_{23}}\left(\frac{\partial^2}{\partial r_{23}^2} + \frac{2}{r_{23}}\frac{\partial}{\partial r_{23}}\right) + \frac{q_1 q_2}{r_{12}} + \frac{q_1 q_3}{r_{13}} + \frac{q_2 q_3}{r_{23}}$$
$$- \frac{1}{m_1}\frac{r_{12}^2 + r_{13}^2 - r_{23}^2}{2 r_{12} r_{13}}\frac{\partial^2}{\partial r_{12}\partial r_{13}} - \frac{1}{m_2}\frac{r_{23}^2 + r_{12}^2 - r_{13}^2}{2 r_{23} r_{12}}\frac{\partial^2}{\partial r_{23}\partial r_{12}} - \frac{1}{m_3}\frac{r_{13}^2 + r_{23}^2 - r_{12}^2}{2 r_{13} r_{23}}\frac{\partial^2}{\partial r_{13}\partial r_{23}}, \tag{10}$$

where m_i and q_i are the mass and charge of particle i,

$$\frac{1}{\mu_{ij}} \equiv \frac{1}{m_i} + \frac{1}{m_j} \tag{11}$$

defines the reduced mass of particles i and j, and, naturally, $r_{ij} = r_{ji}$. Note that the first line contains the contributions of each particle pair to the kinetic energy and the Coulombic potential energy, while the second line contains the kinetic couplings between the particle pairs.

We aim at constructing a NAPES for the degrees of freedom included in the MD, namely, r_{13} and r_{23}. The procedure is analogous to the one presented in Ref. [30], making the correspondences $r_1 \rightarrow r_{13}$, $r_2 \rightarrow r_{23}$, and $r_{12} \rightarrow r_{12}$ and using the Hamiltonian (10) instead of the fixed-nucleus Hamiltonian. Hence, here, we present only the most relevant equations and interpretations and refer the reader to Ref. [30] for further details. Following Hunter [32], we introduce the MCEF of the spatial eigenfunction [30]

$$\Phi(r_{12}, r_{13}, r_{23}) = \psi(r_{13}, r_{23})\chi(r_{12}|r_{13}, r_{23}) \tag{12}$$

by defining marginal and conditional amplitudes

$$\psi(r_{13}, r_{23}) := e^{i\theta(r_{13}, r_{23})}$$
$$\times \left[\int_{|r_{13}-r_{23}|}^{r_{13}+r_{23}} dr_{12}r_{12}|\Phi(r_{12}, r_{13}, r_{23})|^2\right]^{1/2}$$
$$\equiv e^{i\theta(r_{13}, r_{23})}\langle\Phi|\Phi\rangle^{1/2}, \tag{13}$$

$$\chi(r_{12}|r_{13}, r_{23}) := \frac{\Phi(r_{12}, r_{13}, r_{23})}{\psi(r_{13}, r_{23})}, \tag{14}$$

where, from here onwards, angular brackets express integrals over r_{12} with the Jacobian r_{12}. The phase $\exp[i\theta(r_{13}, r_{23})]$, with θ being real, is arbitrary and can be chosen to set the symmetries of ψ and χ with respect to the exchange $r_{13} \leftrightarrow r_{23}$ [30,34]. It can be shown that the marginal amplitude must be

a nodeless (and zeroless) function [30,46]; hence, the conditional amplitude remains finite everywhere. Now we can write

$$D_m(r_{13}, r_{23}) = r_{13}r_{23}|\psi(r_{13}, r_{23})|^2, \tag{15}$$

$$D_c(r_{12}|r_{13}, r_{23}) = r_{12}|\chi(r_{12}|r_{13}, r_{23})|^2, \tag{16}$$

which, together with Eqs. (6)–(8), imply the normalization conditions

$$\int_0^\infty dr_{13}r_{13}\int_0^\infty dr_{23}r_{23}\langle\Phi|\Phi\rangle = 1, \tag{17}$$

$$\int_0^\infty dr_{13}r_{13}\int_0^\infty dr_{23}r_{23}|\psi|^2 = 1, \tag{18}$$

$$\langle\chi|\chi\rangle = 1. \tag{19}$$

The local normalization of χ, Eq. (19), guarantees that the MCEF (12) is unique, within the arbitrary phase mentioned above [34].

To derive the equations that govern ψ and χ we apply the variational principle, as follows. First, we set up the constrained functional [30,34]

$$F[\Phi] \equiv \int_0^\infty dr_{13}r_{13}\int_0^\infty dr_{23}r_{23}\langle\Phi|\hat{H}|\Phi\rangle$$
$$- \int_0^\infty dr_{13}r_{13}\int_0^\infty dr_{23}r_{23}\lambda(r_{13}, r_{23})(\langle\chi|\chi\rangle - 1)$$
$$- \epsilon\left(\int_0^\infty dr_{13}r_{13}\int_0^\infty dr_{23}r_{23}|\psi|^2 - 1\right), \tag{20}$$

where the first term is the expectation value of the energy, the second term enforces the local normalization of χ, and the third term enforces the normalization of ψ, with $\lambda(r_{13}, r_{23})$ and ϵ being Lagrange multipliers. Then we impose the extremization condition $\delta F = 0$, which yields [30]

$$[\hat{T}_{13,23} + U(r_{13}, r_{23})]\psi(r_{13}, r_{23}) = E\psi(r_{13}, r_{23}), \tag{21}$$

$$\hat{\Omega}[\psi]\chi(r_{12}|r_{13}, r_{23}) = U(r_{13}, r_{23})\chi(r_{12}|r_{13}, r_{23}), \tag{22}$$

where

$$\hat{T}_{13,23} \equiv -\frac{1}{2\mu_{13}}\left(\frac{\partial^2}{\partial r_{13}^2} + \frac{2}{r_{13}}\frac{\partial}{\partial r_{13}}\right) - \frac{1}{2\mu_{23}}\left(\frac{\partial^2}{\partial r_{23}^2} + \frac{2}{r_{23}}\frac{\partial}{\partial r_{23}}\right), \tag{23}$$

$$\hat{\Omega}[\psi] \equiv \hat{H} - \frac{1}{\mu_{13}} \frac{1}{\psi} \frac{\partial \psi}{\partial r_{13}} \frac{\partial}{\partial r_{13}} - \frac{1}{\mu_{23}} \frac{1}{\psi} \frac{\partial \psi}{\partial r_{23}} \frac{\partial}{\partial r_{23}}$$
$$- \frac{1}{m_1} \frac{r_{12}^2 + r_{13}^2 - r_{23}^2}{2r_{12}r_{13}} \left(\frac{1}{\psi} \frac{\partial \psi}{\partial r_{13}} \frac{\partial}{\partial r_{12}} \right) - \frac{1}{m_2} \frac{r_{12}^2 + r_{23}^2 - r_{13}^2}{2r_{12}r_{23}} \left(\frac{1}{\psi} \frac{\partial \psi}{\partial r_{23}} \frac{\partial}{\partial r_{12}} \right)$$
$$- \frac{1}{m_3} \frac{r_{13}^2 + r_{23}^2 - r_{12}^2}{2r_{13}r_{23}} \left(\frac{1}{\psi} \frac{\partial \psi}{\partial r_{23}} \frac{\partial}{\partial r_{13}} + \frac{1}{\psi} \frac{\partial \psi}{\partial r_{13}} \frac{\partial}{\partial r_{23}} + \frac{\partial^2 \psi}{\partial r_{13} \partial r_{23}} \right), \tag{24}$$

and the notation $\hat{\Omega}[\psi]$ indicates that this operator depends on $\psi(r_{13}, r_{23})$. The eigenvalues E and $U(r_{13}, r_{23})$ are related to the Lagrange multipliers and to each other by [30]

$$E = \epsilon = \int_0^\infty dr_1 r_1 \int_0^\infty dr_2 r_2 \lambda(r_{13}, r_{23}), \tag{25}$$

$$U(r_{13}, r_{23}) \equiv \frac{\lambda(r_{13}, r_{23})}{|\psi(r_{13}, r_{23})|^2} - \frac{\hat{T}_{13,23} \psi(r_1, r_2)}{\psi(r_{13}, r_{23})}. \tag{26}$$

We have conveniently arranged Eqs. (21) and (22) to expose their analogy with the BO vibrational and clamped-nuclei electronic equations, respectively: r_{12} and $\{r_{13}, r_{23}\}$ are analogous to the electronic and nuclear coordinates, respectively; $\hat{\Omega}[\psi]$ and $\hat{T}_{13,23}$ are analogous to the clamped-nuclei Hamiltonian and the nuclear kinetic-energy operator, respectively; χ and ψ are analogous to the electronic and vibrational eigenfunctions, respectively; and $U(r_{13}, r_{23})$ is analogous to the BO PES, which is the sought-after NAPES. It must be kept in mind that, due to the uniqueness of the MCEF, there can be only one marginal (vibrational) eigenfunction with total energy E associated with this NAPES, in contrast to the BO case, where the same PES can support a number of vibrational states with different total energies. It is very significant that our two main interpretive tools, the MD and the NAPES, turn out to be rigorously related by Eq. (21) together with Eq. (15). In fact, we can regard Eq. (21) as a Schrödinger equation with potential $U(r_{13}, r_{23})$ and eigenfunction $\sqrt{D_m(r_{13}, r_{23})}/r_{13}, r_{23}$. This NAPES can be interpreted as the effective potential acting between the single particle and each of the two identical particles in the mean field of the relative motion between the two identical particles. We emphasize that such an effective potential is exact, in contrast to the BO approximation, where to account for nonadiabatic effects at least two PESs must be coupled. In particular, for an atomlike system Eq. (21) has the form of an *exact* central-field model, with $U(r_{13}, r_{23})$ being the effective radial potential [30]. The definition of our NAPES is in the same spirit as those of Hunter [32] and Gross and coworkers [34,35], which use the full molecular Hamiltonian, but differs from that of Wilson [3,33], which uses the electronic Hamiltonian. Besides their use as interpretive tools for structural problems, Gross and coworkers have used time-dependent NAPESs extensively for the interpretation of coupled electron-nuclear dynamics under time-dependent fields (see, e.g., Ref. [35]).

IV. CALCULATIONS AND DISCUSSION

We studied the atomlike-moleculelike transition of the ground state along a sequence of systems composed of three singly charged fermions. Such a state ought to be a singlet ($S = 0$) with respect to the total spin of the two identical particles, which implies that the spatial eigenfunction (12) must be symmetric with respect to the exchange $r_{13} \leftrightarrow r_{23}$. We set $\theta \equiv 0$, so that both ψ and χ are also symmetric [see Eqs. (13) and (14)].

We considered the sequence of realistic, albeit most of them are exotic, systems H$^-$ ($e^-e^-p^+$), Mu$^-$ ($e^-e^-\mu^+$), Ps$^-$ ($e^-e^-e^+$), Mu$_2^+$ ($\mu^+\mu^+e^-$), H$_2^+$ ($p^+p^+e^-$), where Ps stands for positronium (e^+e^-). [Note that Ps$^-$ and Ps$_2^+$ ($e^+e^+e^-$) are equivalent for our purposes.] He ($e^-e^-\alpha^{2+}$) is not included in this sequence since the alpha particle is doubly charged. We discussed its NAPES and distribution functions in detail in Ref. [30]. Here, we make reference to this system when it helps illuminate the discussion. Since in the sequence ($e^\pm, \mu^\pm, p^\pm$) the mass changes too abruptly, in order to visualize the transition in a smoother way we also considered a series of model systems within a relatively narrow range of the parameter $R \equiv m_s/m_d$, where m_s and m_d are the masses of the single and double particles, respectively.

From a practical standpoint, solving the nonlinear system of Eqs. (21) and (22) does not seem any easier than solving the original Schrödinger equation (9) [47,48]. Since we use these equations for the purposes of analysis, not to obtain solutions of the latter, our strategy consists of extracting approximate marginal and conditional amplitudes from a variationally optimized wave function using Eqs. (13) and (14) and then evaluating the NAPES by

$$U(r_{13}, r_{23}) = \langle \chi | \hat{\Omega}[\psi] | \chi \rangle, \tag{27}$$

in accordance with Eq. (22).

We employed the trial function of Flores-Riveros and Rivas-Silva [49]

$$\Phi(r_{13}, r_{23}, r_{12}) = N(e^{-\alpha r_{13} - \beta r_{23}} + e^{-\beta r_{13} - \alpha r_{23}})$$
$$\times e^{-\gamma(r_{12}-u_0)^2} r_{12}^l, \tag{28}$$

where $\alpha, \beta, \gamma, u_0 \in \mathbb{R}^+$, and $l \in \mathbb{Z}^{0+}$ are variational parameters and N is the normalization factor. We selected this simplistic trial function because it is amenable to a clear physical interpretation. Namely, for atomlike systems the first factor has the form of the Hylleraas unrestricted (different orbitals for different electrons) ansatz for the two-electron atom [40]. On the other hand, to interpret this factor for moleculelike systems let us take α as the larger of the two exponential parameters. Then, when α is sufficiently larger than β so that the exponentials that contain β remain close to 1 in the range where the accompanying exponentials containing α decay to nearly zero, the function resembles the simple linear combination of atomic orbitals–molecular orbital (LCAO-MO) approximation, $1s_1(r_{13}) + 1s_2(r_{23})$, of the

TABLE I. Optimized variational parameters in the trial function (28) for the realistic systems. α, β, γ, and u_0 are given in atomic units.

	$R = m_s/m_d$	α	β	γ	β/γ	u_0	l
He	7294	2.20740	1.41173	0.03253	43.4	4.45774	0
H^-	1836	1.07324	0.47322	0.00957	49.4	11.49397	0
Mu^-	206.8	1.06758	0.46882	0.00957	49.0	11.41274	0
Ps^-	1.000	0.52109	0.15209	0.00744	20.4	8.18378	0
Mu_2^+	0.004836	1.11320	0.21525	1.32386	0.16	1.76860	2
H_2^+	0.000540	1.12988	0.21672	4.87807	0.044	1.93988	2

$1\sigma_g$ MO [44]. The second factor is a ground-state harmonic-oscillator-type eigenfunction that describes vibrational motion along r_{12} about the equilibrium distance u_0. For atomlike systems it plays the role of a Gaussian geminal correlation factor, while for moleculelike systems it represents the harmonic vibration of the nuclei. The third factor introduces anharmonicity into that motion when $l > 0$. Moreover, the evolution of the variational parameters with R aids in the characterization of the transition, as follows. The overall extension of the system is controlled by β: the smaller the value of β is, the larger the extension is. On the other hand, the relative localization of the two identical particles within a given system is controlled by γ: the larger γ is, the higher the localization is. We can claim that the degree of this localization, in comparison with the overall extension, is indicative of the atomlike or moleculelike character of the system since we know that the interelectronic motion in the atom is relatively loose, whereas the internuclear motion in the molecule is relatively rigid. Therefore, we can employ the ratio β/γ as a diagnostic of the progress of the transition along the sequence of systems. In particular, we expect this ratio to decrease as the system becomes more molecule-like.

A further advantage of the trial function (28) is that all of our calculations can be done analytically, which we achieved with the aid of Wolfram *Mathematica* 12.0 [50]. Nevertheless, the expressions are extremely formidable, so we will not show them here.

Table I displays the optimal values of the variational parameters for the sequence of realistic systems (He is included for comparison purposes). It is seen that for the atomic systems Mu^- and H^- ($R \gg 1$) $\alpha \simeq 2\beta$, with $\alpha > 1$. A common interpretation of this relationship is that the atom has an inner electron suffering a negative screening, which makes it more strongly bound than the outer electron suffering a positive screening [39,40]. On the other hand, for the molecular systems Mu_2^+ and H_2^+ ($R \ll 1$) $\alpha \simeq 5\beta$, in accordance with the LCAO-MO interpretation given above. (For H_2^+, it is pertinent to note that our results for α, β, and u_0 are close to the values $\alpha = 1.24$ bohr^{-1}, $\beta \equiv 0$, and $R_e = 2.00$ bohrs obtained from the simple LCAO-MO treatment [44].) Finally, for Ps^- ($R = 1$) $\alpha \simeq 3.4\beta$, so this system can be expected to be somewhat intermediate between atomic and molecular. In addition, for systems with $R > 1$ or $R < 1$, it is found that $l = 0$ or $l = 2$, respectively, which means that in the atomic systems the interelectronic motion is harmonic, whereas in the molecular systems the internuclear motion is anharmonic. Furthermore, it is seen that along the sequence β/γ decreases

(recall that He does not belong in this sequence), as predicted above, and that for the atomic systems $\beta/\gamma \gg 1$, whereas for the molecular systems $\beta/\gamma \ll 1$.

Table II presents the expectation value of the energy obtained from the trial function (28) and the "exact" nonrelativistic energy for the realistic systems. The level of agreement is sufficient for our largely qualitative analysis. Employing more accurate trial functions (see, e.g., Ref. [29]) does not produce any relevant qualitative changes in the features of the NAPESs, MDs, and CDs that will be discussed below, as demonstrated in Ref. [30] (a similar observation was made for the extracule densities in Ref. [21]) and might instead obscure the interpretation.

Table III shows the optimal values of the variational parameters for the sequence of model systems, characterized by $R = m_s$ since the mass of the double particle was kept at $m_d = 1$ atomic unit. It is observed that as R goes from 2.000 to 0.150 (a much smaller range than the one considered in Table I), the ratio α/β goes smoothly from 3.0 to 4.6, the same increasing trend seen in Table I, associated with the transition from the atomlike to moleculelike shape. In addition, for the atomlike systems ($R > 1$) the equilibrium "interelectronic" distance u_0 increases slightly with the mass of the "nucleus" m_s. This is due to the fact that as the nucleus becomes less mobile, it is a little less effective at screening the electrons from one another. On the other hand, for the moleculelike systems ($R < 1$) the equilibrium "internuclear" distance u_0 decreases rather strongly with the mass of the "electron" m_s. This is due to the fact that as the electron becomes less mobile, it is more effective at binding the nuclei. Moreover, it can be seen that across the transition β/γ decreases monotonically (from 27.3 to 11.3), as expected from the previous discussion.

Table IV displays the expectation value of the energy for the model systems. It is observed that as the mass of the single particle decreases, $\langle E \rangle$ increases monotonically; that is, the system becomes less stable. This can be attributed to the increase in the contribution of the single particle to the kinetic energy [see Eq. (10)].

Figure 1 shows the NAPESs for the sequence of realistic systems, and Table II contains data about the relevant topographical features of these surfaces. It is appreciated that for H^-, Mu^-, and Ps^- they resemble that for He discussed in Ref. [30]. In particular, they exhibit two perpendicular basins, separated by a ridge along the $r_{13} = r_{23}$ diagonal which goes asymptotically to zero. A classical interpretation of the topography of such a surface implies that the minima correspond to two broken-symmetry indistinguishable equilibrium configurations (so-called versions [18]) with an inner electron and an

TABLE II. Realistic systems. E_{exact} is the "exact" energy (the sources of these values can be found in Ref. [49]); $\langle E \rangle$ is the energy expectation value; U_e, $U^{\ddagger}$, and $(r_{13,e}, r_{23,e})$ are the energy of the minima, the energy of the saddle point, and the coordinates of a minimum (the coordinates of the other minimum are obtained by interchanging these values) in the NAPES, respectively; and $(r_{13,m}, r_{23,m})$ are the coordinates of the maximum ($r_{13,m} = r_{23,m}$) or one of the maxima ($r_{13,m} \neq r_{23,m}$; the coordinates of the other maximum are obtained by interchanging these values) in the MD. All values are given in atomic units.

	E_{exact}	$\langle E \rangle$	U_e	$U^{\ddagger}$	$r_{13,e}, r_{23,e}$	$r_{13,m}, r_{23,m}$
He	−2.903	−2.902	−7.601	−7.286	0.26, 0.43	0.61, 0.61
H^-	−0.527	−0.525	−1.594	−0.992	0.48, 12.09	1.54, 1.54
Mu^-	−0.525	−0.523	−1.586	−0.986	0.49, 12.03	1.55, 1.55
Ps^-	−0.262	−0.260	−0.792	−0.416	0.99, 11.72	3.26, 3.31
Mu_2^+	−0.585	−0.583	−3.829	−2.065	0.35, 2.20	0.76, 1.99
H_2^+	−0.597	−0.596	−7.544	−4.484	0.25, 2.05	0.75, 1.71

outer electron [39,40]. The saddle point that separates the two basins along the minimum-potential-energy path corresponds to a symmetric configuration with the two electrons on the same orbit. On the other hand, the NAPESs for Mu_2^+ and H_2^+ exhibit two nearly parallel basins originating at relatively narrow wells and separated by a plateau centered at the $r_{13} = r_{23}$ diagonal that approaches zero asymptotically. Interestingly, when the internuclear repulsion is removed from $\hat{\Omega}$ [see Eqs. (24) and (27)], these NAPESs change very little, in contrast to the atomic case, where removal of the interelectronic repulsion from $\hat{\Omega}$ causes the ridge to disappear [30]. In a classical interpretation of this topography, the minima correspond to two versions of a broken-symmetry equilibrium configuration, where one of the nuclei orbits the electron more closely than the other. These two minima are separated by a saddle point that corresponds to a symmetric configuration with the two nuclei remaining at the same distance from the electron. Evidently, for a moleculelike system this NAPES provides explicit information about the relative motion between each nucleus and the electron, with the internuclear motion averaged out, in contrast to the customary BO potential-energy *curve*, which provides explicit information about the internuclear motion in the mean field of the electron [44].

To envision classical motion over such a NAPES, only trajectories with total energy $\langle E \rangle$ ($\simeq E$) are allowed. In addition, since the wave function (28) is symmetric with respect to the exchange $r_{13} \leftrightarrow r_{23}$, such motion must be constituted

by in-phase breathings of the orbits at all times. For example, in the atomic case a straight trajectory running along a basin is permitted, as it corresponds to one orbit breathing along r_{i3} with the other one frozen at $r_{j3} = \text{const}$. In the molecular case, on the other hand, a straight trajectory running along a basin involves an in-phase breathing of both orbits since the basins run nearly along diagonals, which corresponds to a symmetric vibrational mode. In both cases, as the total energy lies above the saddle point (see Table II), the two versions can actually interconvert via trajectories that cross the $r_{13} = r_{23}$ diagonal (a so-called degenerate rearrangement [18]). In the atomic case the asymptotic limit along a basin ($r_{j3} = \text{const}$, $r_{i3} \rightarrow \infty$) would correspond to ionization with the other electron's orbit frozen, while in the molecular case the asymptotic limit along a basin ($r_{13}, r_{23} \rightarrow \infty$) would correspond to a complete breakup of the system, but these limits are, in fact, unreachable since the state is bound.

Figure 1 also displays the corresponding MDs for the realistic systems, and Fig. 2 shows the MD for the He atom for comparison purposes. It is helpful to imagine D_m "sitting" on U. It is seen that for He, H^-, and Mu^- such a distribution is unimodal, with its maximum located on the diagonal, i.e., with both electrons on the same orbit, whereas for Mu_2^+

TABLE III. Optimized variational parameters in the trial function (28) for the model systems. α, β, γ, and u_0 are given in atomic units. $l = 0$ in all cases.

$R = m_s$	α	β	γ	u_0
2.000	0.69797	0.23174	0.00850	8.20320
1.750	0.66546	0.21561	0.00836	8.05929
1.500	0.62658	0.19699	0.00810	8.02482
1.250	0.57969	0.17637	0.00801	7.95740
1.000	0.52109	0.15209	0.00744	8.18378
0.750	0.44661	0.12358	0.00685	8.59581
0.500	0.34870	0.08771	0.00608	9.49008
0.375	0.28541	0.07078	0.00501	11.38755
0.250	0.21056	0.04927	0.00390	14.45530
0.150	0.13915	0.03016	0.00266	19.74359

TABLE IV. Model systems. $\langle E \rangle$ is the energy expectation value, $(r_{13,m}, r_{23,m})$ are the coordinates of the maximum ($r_{13,m} = r_{23,m}$) or one of the maxima ($r_{13,m} \neq r_{23,m}$; the coordinates of the other maximum are obtained by interchanging these values) in the MD, and SD is the second derivative at the maximum or at the middle point between the two maxima of the MD cuts in Fig. 4. All values are given in atomic units.

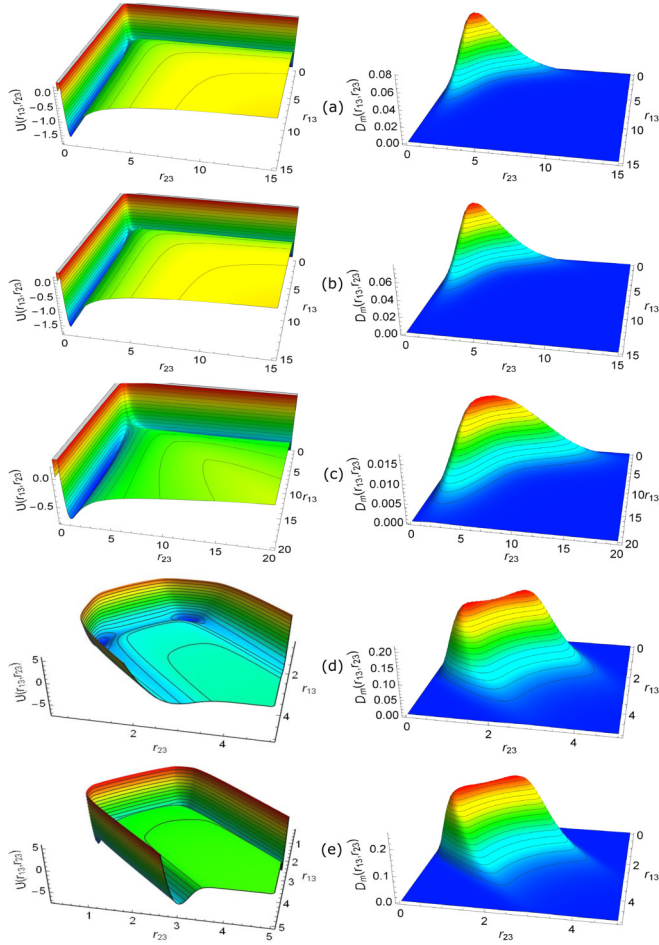| $R = m_s$	$\langle E \rangle$	$r_{13,m}, r_{23,m}$	SD
2.000	−0.346	2.43, 2.43	−0.002059
1.750	−0.330	2.55, 2.55	−0.001446
1.500	−0.311	2.72, 2.72	−0.000821
1.250	−0.288	2.94, 2.94	−0.000320
1.000	−0.260	3.26, 3.31	0.000022
0.750	−0.223	3.39, 4.40	0.000250
0.500	−0.174	3.84, 6.47	0.000274
0.375	−0.144	4.46, 8.43	0.000170
0.250	−0.106	5.73, 11.92	0.000071
0.150	−0.070	8.39, 17.44	0.000018

FIG. 1. NAPESs (left column) and corresponding MDs (right column) for the realistic systems. (a) H^-, (b) Mu^-, (c) Ps^-, (d) Mu_2^+, and (e) H_2^+. All quantities are given in atomic units.

and H_2^+ such a distribution is bimodal, with each maximum located more or less on top of a well (see Table II). Hence, the symmetry breaking implied by the NAPES topography is frustrated in the quantal shape of the atomlike systems (that is, there is no inner-outer separation of the electrons), while
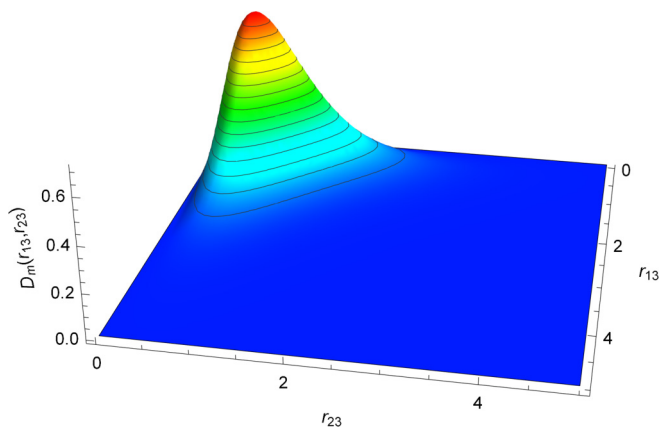
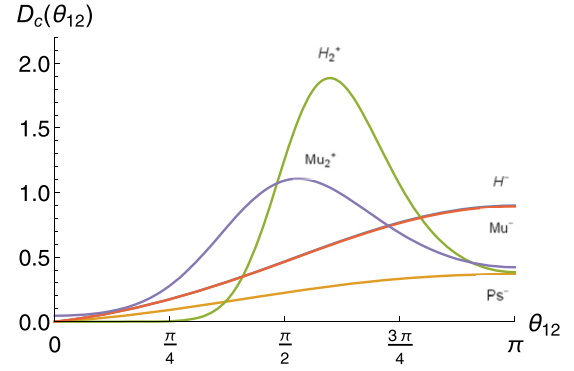FIG. 2. MD for the He atom. All quantities are given in atomic units.

FIG. 3. CDs for the realistic systems evaluated at the maximum or one of the maxima of the corresponding MD for the atomlike or moleculelike cases, respectively.

it is manifested in the quantal shape of the moleculelike systems. (Interestingly, a similar symmetry breaking arises in a fictitious model of He as the *interelectronic repulsion* is enhanced [30].) Evidently, this symmetry breaking in the moleculelike systems is far from sharp, in the sense that configurations in which one of the nuclei orbits the electron closer than the other are only slightly preferred over configurations in which both nuclei are on the same orbit. The fact that the probability of finding the electron at the same distance from the two nuclei is less than the probability of finding it closer to one of the nuclei is in accordance with the well-known characteristics of the covalent bond in H_2^+ [44]. In the case of Ps^-, the MD turns out to be slightly bimodal (see Table II); that is, this system is more moleculelike than atomlike, despite the topography of its NAPES. Moreover, the MD for Ps^- is more spread out than those of H^- and Mu^- since Ps^- is more weakly bound, and the MD for He is much more compact than those for H^- and Mu^-, as the nucleus of the former is doubly charged, whereas the nuclei of the latter are singly charged. These results are in general qualitative agreement with the behavior of the extracule densities reported in Ref. [21]. We must point out that the symmetry breaking in the classical structure implied by the topography of the NAPES and in the quantal shape of the MD is topological [20], in contrast to the symmetry breaking associated with a quantum phase transition across a critical point in the eigenspectrum of the system [51].

Because of the marginalization over r_{12}, the NAPES and MD do not provide explicit information about the correlation between the two identical particles. This kind of information can be retrieved from the CD (16). However, the latter provides radial information, while it is more revealing to examine the angular behavior. Therefore, we transformed $D_c(r_{12}|r_{13}, r_{23})$ into $D_c(\theta_{12}|r_{13}, r_{23})$, where θ_{12} is the angle between the lines joining each of the identical particles with the single particle, by means of the relation $r_{12} = (r_{13}^2 + r_{23}^2 - 2r_{13}r_{23} \cos \theta_{12})^{1/2}$. Figure 3 shows the CDs for the realistic systems, evaluated at the maximum or one of the maxima ($r_{13,m}, r_{23,m}$ in Table II) of the corresponding MD for the atomic or molecular cases, respectively. For the atomic systems, H^- and Mu^-, the CDs are almost identical and increase monotonically from the collinear nucleus-electron-electron
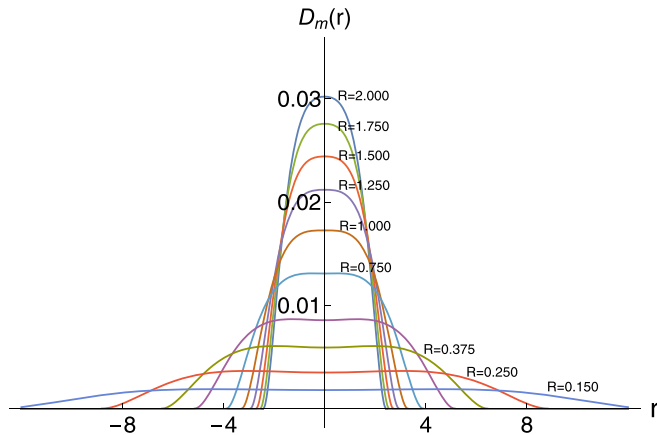
FIG. 4. Cuts of the MDs through the line perpendicular to the diagonal ($r_{13} = r_{23}$) and passing through the maximum or maxima for the model systems (see Table IV). r is the distance from the diagonal. All quantities are given in atomic units.

FIG. 5. Second derivatives at the middle points of the cuts in Fig. 4.

($\theta_{12} = 0$) configuration to the collinear electron-nucleus-electron ($\theta_{12} = \pi$) configuration. The minimum at $\theta_{12} = 0$ reveals the so-called Coulomb hole. The probability of finding the electrons at zero separation is identically zero because the MD maximum is on the $r_{13} = r_{23}$ diagonal and hence the Jacobian present in Eq. (16) $r_{12} = 0$ when $\theta_{12} = 0$. For the molecular systems, Mu_2^+ and H_2^+, the CDs have a maximum at $\simeq 90°$ and $\simeq 110°$, respectively; that is, at this point in the $\{r_{13}, r_{23}\}$ subspace the most probable configuration is bent. The probability of finding the system in the collinear nucleus-nucleus-electron configuration ($\theta_{12} = 0$) now cannot be identically zero because the MD maxima are off the $r_{13} = r_{23}$ diagonal, although for H_2^+ it is practically zero. For Ps^-, the CD is monotonic, albeit much flatter than those of H^- and Mu^-, indicating that this system is more delocalized, in accordance with the larger extension of its MD (see Fig. 1). These results are in general qualitative agreement with the angular densities reported in Ref. [21], except that there that of Ps^- appears slightly nonmonotonic, but care must be taken with a direct comparison since those quantities and our CDs are defined differently. In particular, the CDs shown in Fig. 3 are evaluated at specific points of the $\{r_{13}, r_{23}\}$ subspace; their behaviors at other points are different, although not drastically [30].

In Fig. 1 the change in behavior from atomlike to molecule-like is too sudden due to the abrupt change in the mass ratio (see Table I). In order to visualize the transition in a smoother fashion Fig. 4 displays cuts of the MDs through the line perpendicular to the diagonal $r_{13} = r_{23}$ and passing through the single maximum ($R > 1$) or both maxima ($R < 1$) for the series of model systems (see Table IV). It is seen that as $R = m_s$ decreases, such a cut becomes more spread out and that at around $R = 1$ it smoothly changes shape from unimodal to bimodal. To characterize more quantitatively this transition, we evaluated the second derivative (SD) at the middle point of each cut since, when the curvature at this point is negative or positive, the distribution is unimodal or bimodal, respectively. The results are presented in Table IV and plotted in Fig. 5, where the continuous nature of the transition from
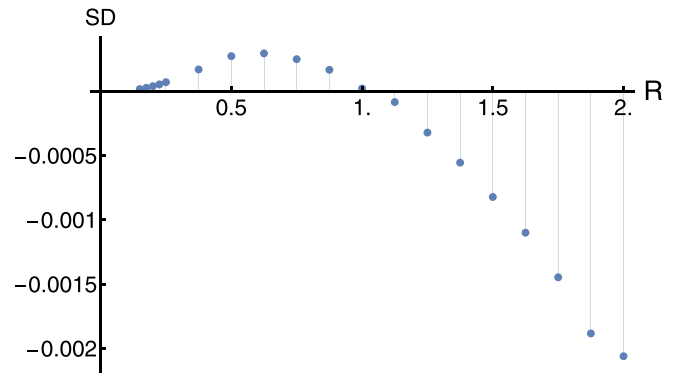
atomlike ($R > 1$, SD < 0) to moleculelike ($R < 1$, SD > 0) can be clearly appreciated. The sign change occurs at $R \simeq 1$ (e.g., Ps^-), which can be taken to mark the boundary between the two types of behaviors. Below $R \approx 0.6$ the magnitude of SD decreases towards zero because the cuts become very spread out.

In Fig. 6 we show the NAPESs and the full MDs for selected model systems. According to Fig. 5, $R = 2$ is the most atomlike system considered, and $R = 0.65, 0.15, 0.05$ are moleculelike, with $R = 0.65$ possessing the highest SD value. It is appreciated how the topography of the NAPES gradually deforms, with the basins initially being close together and perpendicular and at the end being more separated and considerably stretched into the diagonal directions (when making a comparison with Fig. 1, be aware of the different scales). Correspondingly, the MD gradually becomes more extended, with its shape at the same time changing from unimodal to bimodal, with the humps more clearly differentiated and located on top of the wells in the NAPES.

V. CONCLUSIONS AND OUTLOOK

After very briefly reviewing the status of the molecular structure conundrum [1–11,16,19,25,27] and stating our view about the concept of shape for an isolated quantal system, we presented an alternative characterization of the continuous emergence of molecular shape in prototypical three-particle Coulomb systems as a response to the variation of the particle masses solely from the correlations between all the particles being treated on equal footing.

Our analysis was based mainly on the behaviors of the two-dimensional nonadiabatic potential-energy surface and the marginal distribution of the distances between the single particle and each of the two identical particles, constructed rigorously by means of a marginal-conditional exact factorization of a variationally optimized internal wave function. The analysis was further aided by an examination of the evolution of the variational parameters and the conditional distribution of the angle defined by the two identical particles and the single particle. The classical interpretation of the topography of such a surface implies two broken-symmetry indistinguishable equilibrium structures, where both identical particles move around the single particle along separate
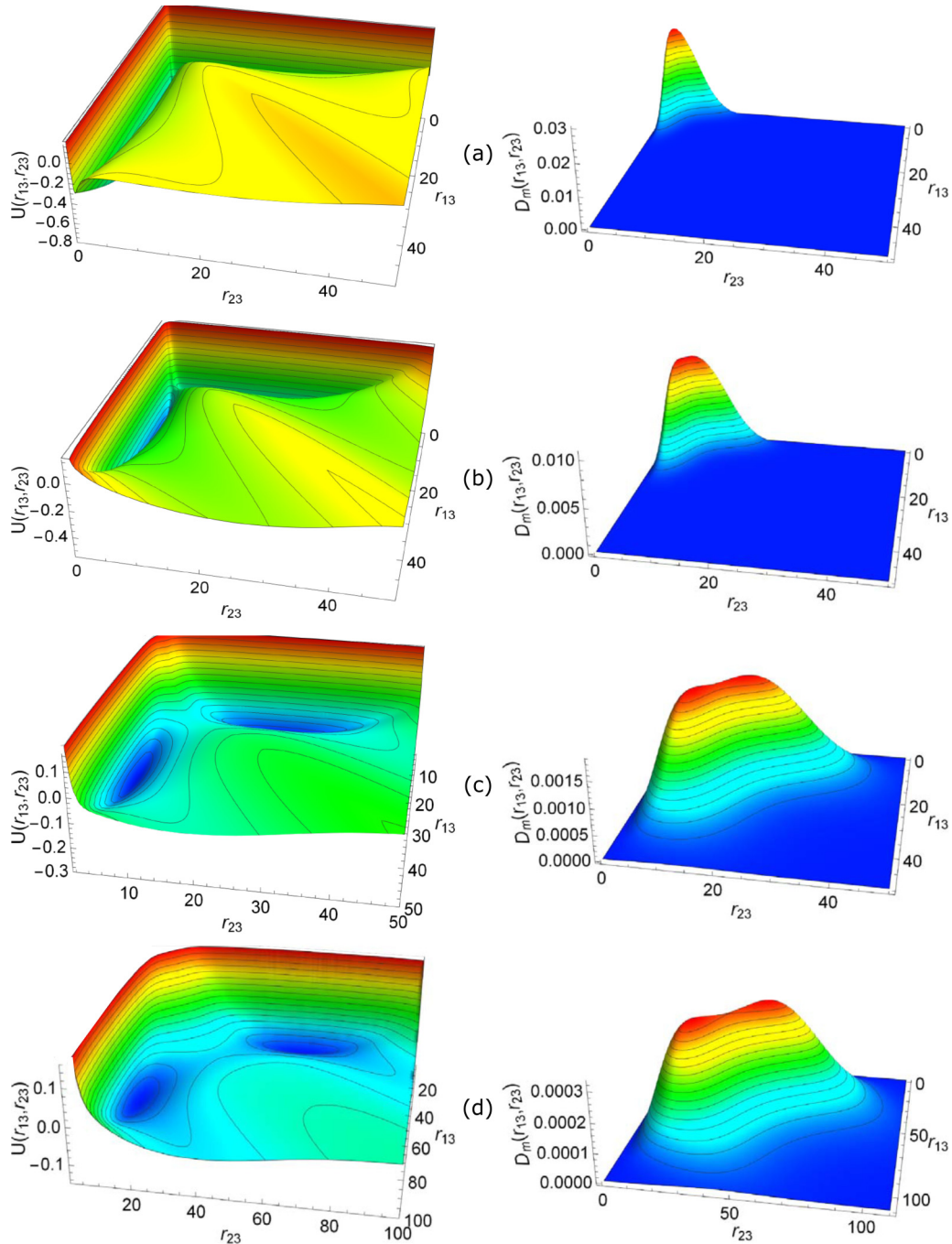
FIG. 6. NAPESs (left column) and corresponding MDs (right column) for selected model systems. (a) $R = 2.00$, (b) $R = 0.65$, (c) $R = 0.15$, and (d) $R = 0.05$. All quantities are given in atomic units.

orbits. Such topological symmetry breaking is frustrated in the atomlike systems but preserved in the moleculelike ones, as revealed by the continuous transition from the unimodal to bimodal shape of the quantal marginal distribution. The conditional distribution, evaluated at selected points of the $\{r_{13}, r_{23}\}$ subspace, turns from monotonic to nonmonotonic with a single maximum across the transition.

The unimodal-bimodal transition has already been observed in cuts of the one-particle extracule densities employed in Refs. [20,21,29]. Our characterization has two advantages: First, it is univocal, as it does not rely on the definition of

a reference point, in contrast to the one-particle extracule densities, where the bimodality is lost for certain choices of reference points [36,37]. Second, it permits a unified treatment of atoms, molecules, and any other collection of quantum particles in terms of the potential-energy-surface concept, which has proven to be a very powerful interpretive tool in quantum chemistry.

For a three-particle system, three alternative marginal-conditional factorizations are possible that will generate one different two-dimensional nonadiabatic potential-energy surface and two nonadiabatic potential-energy *curves*, which,

together with their corresponding marginal and conditional distributions, can be employed to discuss related issues of particle correlation and the nature of the Born-Oppenheimer approximation. In addition, hyperspherical coordinates [52] constitute an attractive alternative to the interparticle distances because the hyperradius R and the angles α and θ_{12} are directly related to the size and the shape of the system, respectively. These investigations are underway in our laboratory.

It has been discovered that certain doubly excited states of two-electron atoms can be empirically modeled in terms of collective rotational- and bendinglike motions of the electrons, analogous to the rovibrational motions of a linear *ABA* molecule [53] (Ref. [45] reviews this development). In addition, it has been predicted that other doubly excited states of two-electron atoms adopt classical-like configurations with both electrons on the same side of the nucleus (so-called frozen-planet states) [54]. Moreover, it is known that molecules in highly excited vibrational states can become fluxional. (For a unified review of these three aspects see Ref. [55]). It is very desirable to develop a unified view of these types of systems [55]. We feel that our methodology will be capable of achieving this goal.

ACKNOWLEDGMENT

[1] R. G. Woolley, Quantum theory and molecular structure, Adv. Phys. **25**, 27 (1976).

[2] R. G. Woolley, Must a molecule have a shape? J. Am. Chem. Soc. **100**, 1073 (1978).

[3] E. B. Wilson, On the definition of molecular structure in quantum mechanics, Int. J. Quantum Chem. **16**, 5 (1979).

[4] P. Claverie and S. Diner, The concept of molecular structure in quantum theory: Interpretation problems, Isr. J. Chem. **19**, 54 (1980).

[5] M. García-Sucre and M. Bunge, Geometry of a quantal system, Int. J. Quantum Chem. **19**, 83 (1981).

[6] H. Primas, *Chemistry, Quantum Mechanics and Reductionism*, 2nd ed. (Springer, Berlin, 1983).

[7] S. J. Weininger, The molecular structure conundrum: Can classical chemistry be reduced to quantum chemistry? J. Chem. Educ. **11**, 939 (1984).

[8] R. G. Woolley, The molecular structure conundrum, J. Chem. Educ. **12**, 1082 (1985).

[9] R. G. Woolley, Molecular shapes and molecular structures, Chem. Phys. Lett. **125**, 200 (1986).

[10] R. G. Woolley, Quantum theory and the molecular hypothesis, in *Molecules in Physics, Chemistry, and Biology*, edited by J. Maruani (Springer, Dordrecht, 1988), Vol. 1, pp. 45–89.

[11] G. Woolley, Must a molecule have shape? New Scientist (London) **120**, 53 (1988).

[12] B. T. Sutcliffe, The chemical bond and molecular structure, J. Mol. Struct.: THEOCHEM **259**, 29 (1992).

[13] B. T. Sutcliffe and R. G. Woolley, On the quantum theory of molecules, J. Chem. Phys. **137**, 22A544 (2012).

[14] B. Sutcliffe and R. G. Woolley, The potential energy surface in molecular quantum mechanics, in *Advances in Quantum Methods and Applications in Chemistry, Physics, and Biology*, edited by M. Hotokka, E. J. Brändas, J. Maruani, and G. Delgado-Barrio (Springer, Cham, 2013), pp. 3–40.

[15] J. D. Mills, J. A. Boatz, and P. W. Langhoff, Quantum-mechanical definition of atoms and their mutual interactions in Born-Oppenheimer molecules, Phys. Rev. A **98**, 012506 (2018).

[16] J. C. Martínez-González, S. Fortin, and O. Lombardi, Why molecular structure cannot be strictly reduced to quantum mechanics, Found. Chem. **21**, 31 (2019).

[17] B. T. Sutcliffe and R. G. Woolley, Is chemistry really founded in quantum mechanics? arXiv:2003.06599.

[18] P. R. Bunker and P. Jensen, *Molecular Symmetry and Spectroscopy*, 2nd ed. (NRC Research Press, Ottawa, 1998).

[19] H. Primas, Emergence in exact natural sciences, Acta Polytechnica Scandinavica **91**, 83 (1998).

[20] E. Mátyus, J. Hutter, U. Müller-Herold, and M. Reiher, On the emergence of molecular structure, Phys. Rev. A **83**, 052512 (2011).

[21] E. Mátyus, J. Hutter, U. Müller-Herold, and M. Reiher, Extracting elements of molecular structure from the all-particle wave function, J. Chem. Phys. **135**, 204302 (2011).

[22] E. Mátyus and P. Cassam-Chenaï, Orientational decoherence within molecules and emergence of the molecular shape, J. Chem. Phys. **154**, 024114 (2021).

[23] P. Cassam-Chenaï and E. Mátyus, Electrons as an environment for nuclei within molecules: A quantitative assessment of their contribution to a classical-like molecular structure, Theor. Chem. Acc. **140**, 159 (2021).

[24] C. Zhong and F. Robicheaux, Decoherence of rotational degrees of freedom, Phys. Rev. A **94**, 052109 (2016).

[25] A. Franklin and V. Seifert, The problem of molecular structure just is the measurement problem, Br. J. Philos. Sci. (to be published).

[26] M. Schlosshauer, *Decoherence and the Quantum-to-Classical Transition* (Springer, Berlin, 2007).

[27] S. Fortin, O. Lombardi, and J. C. Martínez-González, Isomerism and decoherence, Found. Chem. **18**, 225 (2016).

[28] S. Fortin and O. Lombardi, Is the problem of molecular structure just the quantum measurement problem? Found. Chem. **23**, 379 (2021).

[29] A. L. Baskerville, A. W. King, and H. Cox, Quantum effects of nuclear motion in three-particle diatomic ions, Phys. Rev. A **94**, 042512 (2016).

[30] L. D. Salas and J. C. Arce, Potential energy surfaces in atomic structure: The role of Coulomb correlation in the ground state of helium, Phys. Rev. A **95**, 022502 (2017).

[31] E. Mátyus, Pre-Born-Oppenheimer molecular structure theory, Mol. Phys. **117**, 590 (2018).

[32] G. Hunter, Conditional probability amplitudes in wave mechanics, Int. J. Quantum Chem. **9**, 237 (1975).

[33] P. Cassam-Chenaï, On non-adiabatic potential energy surfaces, Chem. Phys. Lett. **420**, 354 (2006).

[34] N. I Gidopoulos and E. K. U. Gross, Electronic non-adiabatic states: Towards a density functional theory beyond the Born-Oppenheimer approximation, Philos. Trans. R. Soc. A **372**, 20130059 (2014).

[35] A. Abedi, N. T. Maitra, and E. K. U. Gross, Correlated electron-nuclear dynamics: Exact factorization of the molecular wavefunction, J. Chem. Phys. **137**, 22A530 (2012).

[36] C. G. Rodríguez, A. S. Urbina, F. J. Torres, D. Cazar, and E. V. Ludeña, Non-Born-Oppenheimer nuclear and electronic densities for a three-particle Hooke-Coulomb model, Comput. Theor. Chem. **1018**, 26 (2013).

[37] M. Becerra, V. Posligua, and E. V. Ludeña, Non-Born-Oppenheimer nuclear and electronic densities for a Hooke-Coulomb model for a four-particle system, Int. J. Quantum Chem. **113**, 1584 (2013).

[38] P. Coppens, *X-Ray Charge Densities and Chemical Bonding* (Oxford University Press, Oxford, 1997).

[39] A. W. King, L. C. Rhodes, and H. Cox, Inner and outer radial density functions in correlated two-electron systems, Phys. Rev. A **93**, 022509 (2016).

[40] E. A. Hylleraas, Neue Berechnung der Energie des Heliums im Grundzustande, sowie des tiefsten Terms von Ortho-Helium, Z. Phys. **54**, 347 (1929); An english translation of this paper can be found in *Quantum Chemistry: Classic Scientific Papers*, translated and edited by H. Hettema (World Scientific, Singapore, 2000).

[41] E. A. Hylleraas, The Schrödinger two-electron atomic problem, Adv. Quantum Chem. **1**, 1 (1964).

[42] A. A. Frost, The use of interparticle coordinates in electronic energy calculations for atoms and molecules, Theor. Chim. Acta **1**, 36 (1962).

[43] A. M. Frolov, Bound-state calculations of Coulomb three-body systems, Phys. Rev. A **59**, 4270 (1999).

[44] I. N. Levine, *Quantum Chemistry*, 7th ed. (Pearson, Upper Saddle River, NJ, 2014).

[45] R. S. Berry, Probing the collective and independent-particle character of atomic electrons, in *Structure and Dynamics of Atoms and Molecules: Conceptual Trends*, edited by J. L. Calais and E. S. Kryachko (Springer, Dordrecht, 1995), pp. 155–181.

[46] G. Hunter, Nodeless wave functions and spiky potentials, Int. J. Quantum Chem. **19**, 755 (1981).

[47] T. Jecko, B. T. Sutcliffe, and R. G. Woolley, On factorization of molecular wavefunctions, J. Phys. A **48**, 445201 (2015).

[48] G. H. Gossel, L. Lacombe, and N. P. Maitra, On the numerical solution of the exact factorization equations, J. Chem. Phys. **150**, 154112 (2019).

[49] A. Flores-Riveros and J. F. Rivas-Silva, Variational description of the 3-body Coulomb problem through a correlated Eckart-Gaussian wavefunction, Braz. J. Phys. **29**, 529 (1999).

[50] Wolfram Research, Inc., *Mathematica*, version 12.0, Champaign, IL, 2020.

[51] Q. Shi and S. Kais, Quantum criticality at the large-dimensional limit: Three-body Coulomb systems, Int. J. Quantum Chem. **85**, 307 (2001).

[52] C. D. Lin, Hyperspherical coordinate approach to atomic and other Coulombic three-body systems, Phys. Rep. **257**, 1 (1995).

[53] M. E. Kellman and D. R. Herrick, Ro-vibrational collective interpretation of supermultiplet classifications of intrashell levels of two-electron atoms, Phys. Rev. A **22**, 1536 (1980).

[54] K. Richter, J. S. Briggs, D. Wintgen, and E. A. Solov'ev, Novel dynamical symmetries of asymmetrically doubly excited two-electron atoms, J. Phys. B **25**, 3929 (1992).

[55] M. E. Kellman, Nonrigid systems in chemistry: A unified view, Int. J. Quantum Chem. **65**, 399 (1997).